Protoplasma (2015) 252:439–450
DOI 10.1007/s00709-014-0689-x

ORIGINAL ARTICLE

Anther ontogeny in *Brachypodium distachyon*

Akanksha Sharma · Mohan B. Singh · Prem L. Bhalla

Received: 28 April 2014 / Accepted: 13 August 2014 / Published online: 23 August 2014

Abstract *Brachypodium distachyon* has emerged as a model plant for the improvement of grain crops such as wheat, barley and oats and for understanding basic biological processes to facilitate the development of grasses as superior energy crops. *Brachypodium* is also the first species of the grass subfamily Pooideae with a sequenced genome. For obtaining a better understanding of the mechanisms controlling male gametophyte development in *B. distachyon*, here we report the cellular changes during the stages of anther development, with special reference to the development of the anther wall. *Brachypodium* anthers are tetrasporangiate and follow the typical monocotyledonous-type anther wall formation pattern. Anther differentiation starts with the appearance of archesporial cells, which divide to generate primary parietal and primary sporogenous cells. The primary parietal cells form two secondary parietal layers. Later, the outer secondary parietal layer directly develops into the endothecium and the inner secondary parietal layer forms an outer middle layer and inner tapetum by periclinal division. The anther wall comprises an epidermis, endothecium, middle layer and the secretory-type tapetum. Major documented events of anther development include the degradation of a secretory-type tapetum and middle layer during the course of development and the rapid formation of U-shaped endothecial thickenings in the mature pollen grain stage. The tapetum undergoes degeneration at the tetrad stage and disintegrates completely at the bicellular stage of pollen development. The distribution of insoluble polysaccharides in the anther layers and connective tissue through progressive developmental stages suggests their role in the development of male gametophytes. Until sporogenous cell stage, the amount of insoluble polysaccharides in the anther wall was negligible. However, abundant levels of insoluble polysaccharides were observed during microspore mother cell and tetrad stages and gradually declined during the free microspore and vacuolated microspore stages to undetectable level at the mature stage. Thus, the cellular features in the development of anthers in *B. distachyon* share similarities with anther and pollen development of other members of Poaceae.

Keywords Anther ontogeny · Anther wall · *Brachypodium* · Poaceae · Microsporogenesis · Tapetum · Male gametophyte development

Introduction

The temperate and wild grass species *Brachypodium distachyon* has emerged as a model plant for grasses and cereal crops in much the same way as *Arabidopsis* has served as a model for dicotyledonous plants (Draper et al. 2001). Due to its small stature (20 cm), rapid life cycle (2–3 months), simple genetic transformation protocol and the availability of complete genome sequence, *Brachypodium* is increasingly being used for structural and functional genomics of grasses (Garvin et al. 2008; Opanowicz et al. 2008; Alves et al. 2009; Bevan et al. 2010). Moreover, *Brachypodium* is a close phylogenetic relative of small temperate grain crops (e.g. wheat, oat and barley) and forage grasses (e.g. rye grass, timothy grass and Kentucky blue grass), with all of these plants belonging to the Pooideae subfamily of the family Poaceae. Despite the ever-increasing interest in *Brachypodium* as a model plant, very little is known about its structural biology of reproduction. Here, we investigated cellular

Handling Editor: Benedikt Kost

A. Sharma · M. B. Singh · P. L. Bhalla (✉)
Plant Molecular Biology and Biotechnology Laboratory, Melbourne School of Land and Environment, University of Melbourne, Parkville, Melbourne, VIC 3010, Australia
e-mail: premlb@unimelb.edu.au

features associated with pollen and anther development in this important model plant species.

In flowering plants, male gametophyte (pollen) development is an important process that results in the formation of sperm cells that are required for the fertilisation of the egg, leading to successful plant sexual reproduction and seed set. Pollen development takes place in the anther and comprises a series of complex events involving interactions between anther tissues (Mascarenhas 1989; Schrauwen et al. 1996). The entire process can be studied in two distinct and successive developmental phases: microsporogenesis and microgametogenesis. During microsporogenesis, the diploid sporogenous cells differentiate as microsporocytes that undergo meiosis and form four haploid unicellular microspores in a tetrad. Microgametogenesis starts with the release of haploid microspores from tetrads, leading to the formation of male gametophytes (Bedinger 1992). Defects in the development of pollen or the surrounding nutritive layer of the anther, the tapetum, can lead to male sterility and failure to set seed (Bhandari 1984; Polowick and Sawhney 1992).

In most angiosperms, the anther is tetrasporangiate and has a four-layered wall. The anther wall is composed of the epidermis, endothecium, middle layer and tapetum. While each layer has a specific presumed function in anther physiology, they act together to contribute towards pollen development (Bhandari 1984). The tapetum is the innermost layer of the anther wall that surrounds the developing gametophytes (Pacini et al. 1985) and provides the exchange of nutritional, structural or regulatory compounds between the sporophytic anther tissues and the developing male gametophytes (Schrauwen et al. 1996). During microsporogenesis, the tapetum performs a secretory role by supplying essential nutrients to the developing microspores, providing enzymes (callase) for callose dissolution to release microspores from tetrads and materials for pollen wall formation (Bedinger 1992). At the time of maturation, the middle layer, and in particular the tapetum, degenerates to facilitate the release of mature pollen (Bhandari 1984; Pacini 1990, 2000). The crucial role of the tapetum in pollen development is highlighted by the fact that male sterility in plants is often associated with tapetal abnormalities (Bhandari 1984; Polowick and Sawhney 1992).

Davis (1996) described four types of anther wall development based on the secondary parietal layers: basic type (type I), dicotyledonous type (type II), monocotyledonous type (type III) and reduced type (type IV). Many authors have followed this classification to explain anther wall ontogeny in different plants (Carrizo Garcia 2002; Hardy and Stevensen 2000; Liu and Huang 2003; Aybeke 2012). In general, one type of anther development is found in each family. However, in some families, two types of anther wall development have been reported, such as in the Solanaceae family, which has type I and type II anther wall development (Carrizo Garcia 2002), and the Commelinaceae family, which has type I and type III anther wall development (Hardy and Stevensen 2000).

The metabolic processes involved in the biosynthesis of nutritional substances such as starch, lipids and proteins are synthesised in anthers and play an important role in pollen development. For instance, interference in the sugar metabolism of the anther could have a detrimental effect on pollen and eventually lead to male sterility (Dorion et al. 1996; Datta et al. 2002). The amount and distribution of these reserve substances vary in anther tissues throughout the developmental process. Despite its potential to contribute to our understanding of reproductive processes in grasses, no study focussing on anther and pollen development in the genus *Brachypodium* is available to date. Therefore, to address this gap, we are focussing on pollen and anther ontogeny in *B. distachyon* at cytochemical and ultrastructural levels. In *B. distachyon*, the stages of anther and pollen development have been correlated to a period of 9 days of spikelet development after the first awn was visible, as described previously, and thus the anther and pollen developmental process was divided into ten stages (Sharma et al. 2014). Here, we report anther ontogeny in *B. distachyon* from archesporial cells to the mature tricellular pollen with a special focus on the differentiation and structure of the anther wall. In addition, the distribution of insoluble polysaccharides (starch) in the anthers of *B. distachyon* was also investigated through ten sequential developmental stages.

Materials and methods

B. distachyon (Bd21-3) plants were grown in a glasshouse under controlled conditions as described by Vogel and Hill (2008). Because a description of growth stages in *B. distachyon* is already available (Hong et al. 2011), development of the spikelet was observed closely from the end of the booting stage, when the first awn was just visible out of the flag leaf, until dehisced anthers were observed. With the onset of the first awn, the spikelet was selected as the day 1 spikelet. From then on, the spikelets were collected on each successive day for 9 days until anthesis (Sharma et al. 2014). Immature spikelets were dissected with the awns removed (1–5 days), and anthers were excised from the base florets of mature spikelets (6–9 days). The entire experiment was conducted over three replicates (Sharma et al. 2014).

Light microscopy

For light microscopy studies, spikelets and anthers were fixed immediately in cold 2.5 % glutaraldehyde/0.1 M PBS (phosphate-buffered saline), pH 7.0, for 4 h at room temperature. After two washes of 30 min each with PBS buffer, the spikelets and anthers were dehydrated in a series of increasing concentration of ethanol in water (30, 50, 70, 80, 90 %) for 1 h each and finally in 100 % ethanol. Spikelets and anthers were then incubated in 1:1 and 1:3 ethanol/resin (LR White) mixtures for 1 day each at room temperature and finally in 100 % resin overnight on a rotating stage. Following dehydration, spikelets and anthers were embedded in LR White, polymerised by incubation at 60 °C for 24–30 h and sliced to 0.5-μm thickness with a Leica Ultracut® microtome.

For cytochemical studies, semi-thin sections were stained with toluidine blue for general morphological observation, with periodic acid-Schiff (PAS) reagent for detecting insoluble carbohydrates such as starch and with DAPI (4′,6-diamino-2-phenylindole) for detecting DNA.

Transmission electron microscopy

For transmission electron microscopy (TEM), thin sections of 90 nm were cut from LR White-embedded material with a Leica Ultracut® microtome and stained with 2 % uranyl acetate for 10 min followed by triple lead stain for 5 min (Sato 1968). Thin sections were examined and micrographs were taken with a Philips CM120 BioTwin transmission electron microscope.

Results

In *B. distachyon* (Fig. 1), the anthers are basifixed and tetrasporangiate. Immature anthers of *B. distachyon* are yellow-green in colour and attached to short filaments (Fig. 1b), whereas mature anthers appear yellow and are attached to elongated filaments (Fig. 1c). The process of anther development was studied throughout microsporogenesis and microgametogenesis and is classified into ten different stages. The related description of major events corresponding to these stages is described in Table 1.

Stage 1: Archesporial cell stage

At the earliest examined stage, the anther appeared cylindrical to ovoid in shape in semithin sections. The anther differentiates with the formation of archesporial cells at the four corners surrounded by a single layer of epidermal cells (Fig. 2a). The archesporial cells appeared slightly larger than epidermal and connective cells (Fig. 2a, b). Cytochemical reactions revealed that epidermal as well as archesporial cells of the anther presented a very faint reaction with regard to insoluble

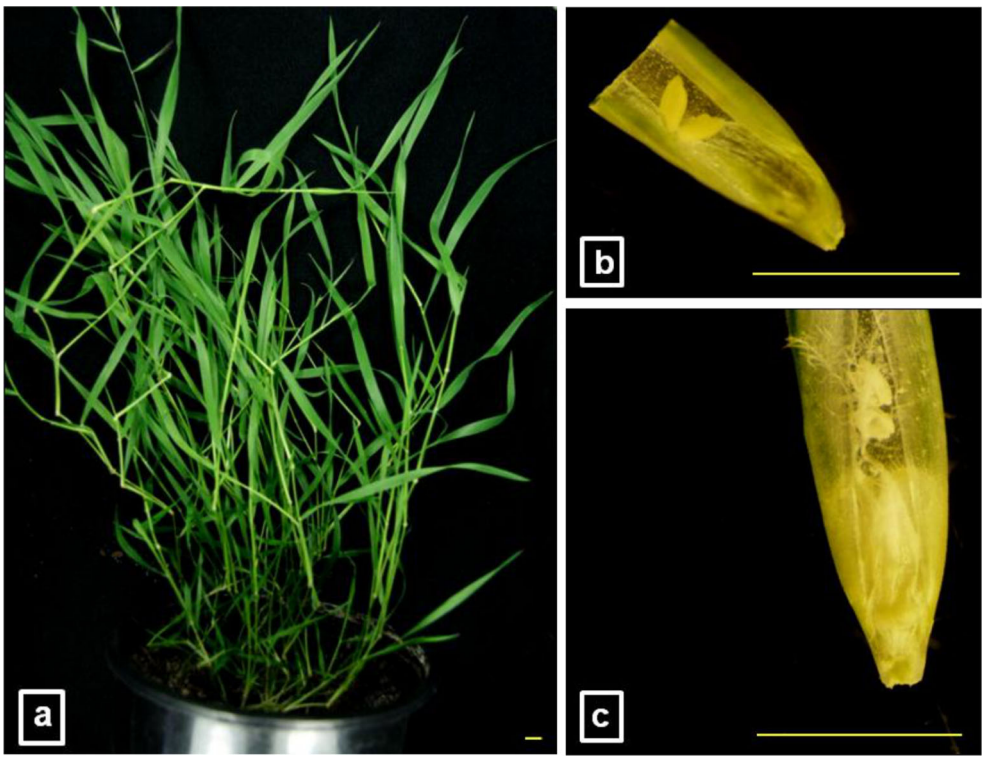

Fig. 1 *B. distachyon* at different stages of flowering. **a** *B. distachyon* plant at flowering stage. **b** Dissected floret showing immature anthers with short filaments. **c** Dissected floret showing mature anthers with elongated filaments. **a** *Bar* 1 cm; **b**, **c** *Bar* 200 μm

Table 1 Major cellular events during *B. distachyon* anther development

Stage	Major events
Archesporial cell stage	Archesporial cells arise in four corners of oval-shaped primordia
Primary parietal cell stage	Archesporial cells divide and differentiate into primary parietal cells
Primary sporogenous cell stage	Cell divisions further generate the secondary parietal layers and primary sporogenous cells. Anther wall differentiates into three layers
Sporogenous cell stage	The primary sporogenous cells divide and form sporogenous cells. The outer secondary parietal layer forms the endothecium layer, and the inner secondary parietal layer develops into the middle layer and the tapetum. Anther differentiates into four layers
Microspore mother cell stage	Formation of microspore mother cells surrounded by four-layered anther wall. Tapetal cells are mostly binucleated
Tetrad stage	Microspore mother cells undergo meiosis, generating four haploid microspores. Middle layer is crushed, and tapetum becomes vacuolated. Anther undergoes a general increase in size
Free microspore stage	Free haploid microspores with thin walls are released. Tapetal cells become condensed and form characteristic Orbicules/Ubisch bodies on the inner surface facing the microspores. The middle layer becomes a less visible band-like structure
Vacuolated microspore stage	Tapetal cells become more degenerated and produce abundant Ubisch bodies. The microspore becomes more vacuolated with a round shape. The middle layer disappears
Bicellular pollen stage	The tapetal cells almost completely degenerate into cellular debris and Ubisch bodies on the internal surface. Epidermal cells form a layer of cuticle, and endothecial cells develop fibrous bands
Mature pollen stage	The tapetum completely disappears. With maturation, only the epidermis and endothecium layers remain intact

polysaccharides as carried out by negative PAS staining (Fig. 2b).

Stage 2: Primary parietal cell stage

Periclinal divisions of archesporial cells generate distinct primary parietal cells (Fig. 3). The primary parietal cells were enclosed in the anther locule, surrounded by an epidermis (Fig. 3c). Small vacuoles and plastids were observed in the cytoplasm of primary parietal cells (Fig. 3d).

Stage 3: Primary sporogenous cell stage

Further periclinal divisions of archesporial cells give rise to primary sporogenous cells (Fig. 4). The primary parietal cells form two secondary parietal layers (Fig. 4a). The newly formed primary sporogenous cell appears quite distinct from the rest of the cells of the anther lobe by its large size and conspicuous nucleus (Fig. 4b, c). Small vacuoles were also observed in the cytoplasm of primary sporogenous cells (Fig. 4c). The developing anther at this stage has characteristic locules, a three-layer anther wall and connective and vascular tissue. Cytochemical staining showed a weak reaction to insoluble polysaccharides in the primary sporogenous cells and anther walls (Fig. 4d).

Stage 4: Sporogenous cell stage

As development progresses, the primary sporogenous cells divide to form sporogenous cells or microsporocytes (Fig. 5a), with the outer secondary parietal layer developing into the endothecium layer. The inner secondary parietal layer undergoes periclinal divisions and forms an outer middle layer and inner tapetum. At this stage of development, the anther has four concentric somatic layers that surround the microsporocytes (listed from the surface to the interior): the epidermis, the endothecium, the middle layer and the tapetum (Fig. 5a–d). The tapetal cells were rectangular in outline, possessed a single large nucleus and were connected to each other by plasmodesmatal connections (Fig. 5b, c). Numerous vacuoles, mitochondria and plastids were observed in cells of all four anther layers (Fig. 5b, c). At this stage, some

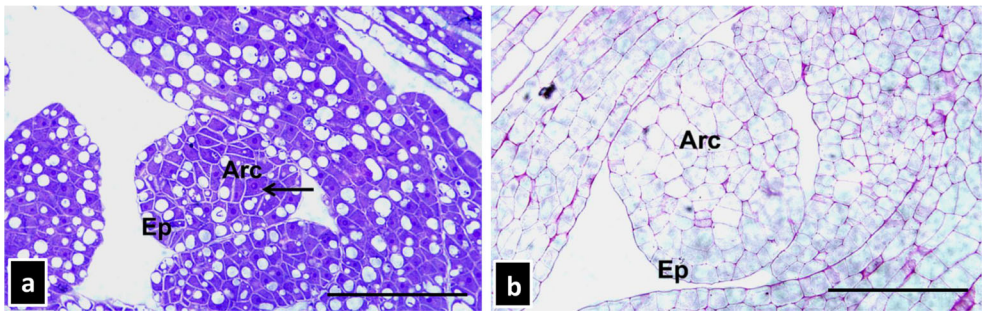

Fig. 2 Anther wall formation in longitudinal sections of spikelets of *B. distachyon* at archesporial cell stage. **a** Undifferentiated anther with archesporial cells (*arrow*). **b** Longitudinal section stained with PAS at archesporial cell stage. Note the archesporial cells and epidermis showing negative staining for insoluble polysaccharides. *Arc* archesporial cell, *Ep* epidermis. *Bar* 50 μm

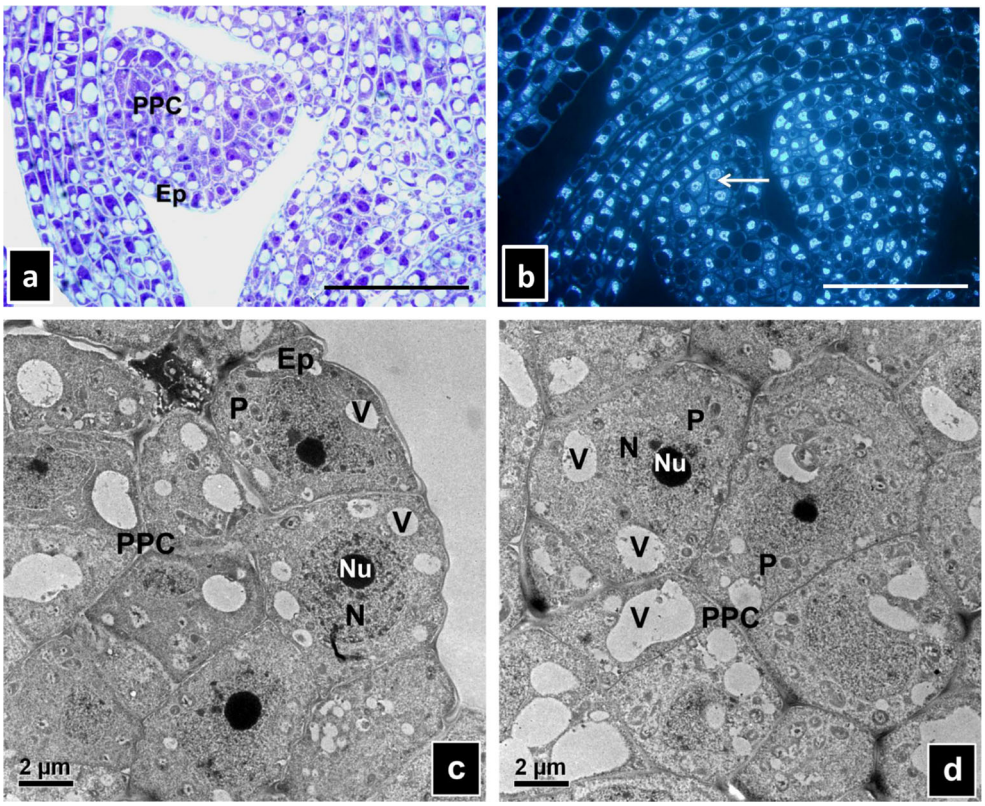

Fig. 3 Light, fluorescent and TEM micrographs of longitudinal sections of spikelets at primary parietal cell stage. **a** Semi-thin section stained with toluidine blue showing primary parietal cells surrounded by a single row of epidermal cells. **b** Semi-thin section stained with DAPI. Note the presence of evident nuclei of primary parietal cells (*arrow*). **c** Ultrastructure of epidermis surrounding primary parietal cells. **d** Ultrastructure of primary parietal cells. *Ep* epidermis, *PPC* primary parietal cells, *N* nucleus, *Nu* nucleolus, *V* vacuole, *P* plastid. Light micrographs: *bar* 50 µm

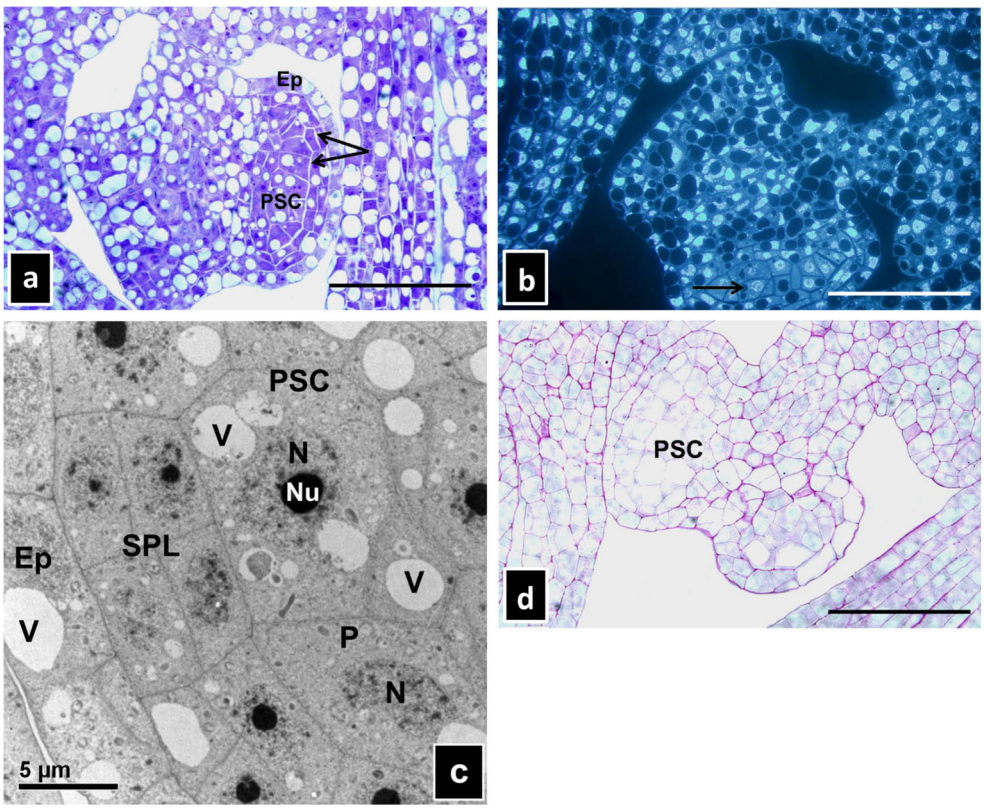

Fig. 4 Light, fluorescent and TEM micrographs of longitudinal sections of spikelets at primary sporogenous cell stage. **a** Semi-thin section stained with toluidine blue. Note the two secondary parietal layers (*arrows*). **b** Semi-thin section stained with DAPI. Note the evident nuclei of primary sporogenous cells (*arrow*). **c** Ultrastructure of primary sporogenous cells surrounded by three-layered anther wall. **d** Longitudinal section stained with PAS. Note the absence of insoluble polysaccharides in primary sporogenous cells and anther layers as evident by negative PAS staining. *Ep* epidermis, *PSC* primary sporogenous cells, *SPL* secondary parietal layers, *N* nucleus, *Nu* nucleolus, *V* vacuole, *P* plastid. Light micrographs: *bar* 50 µm

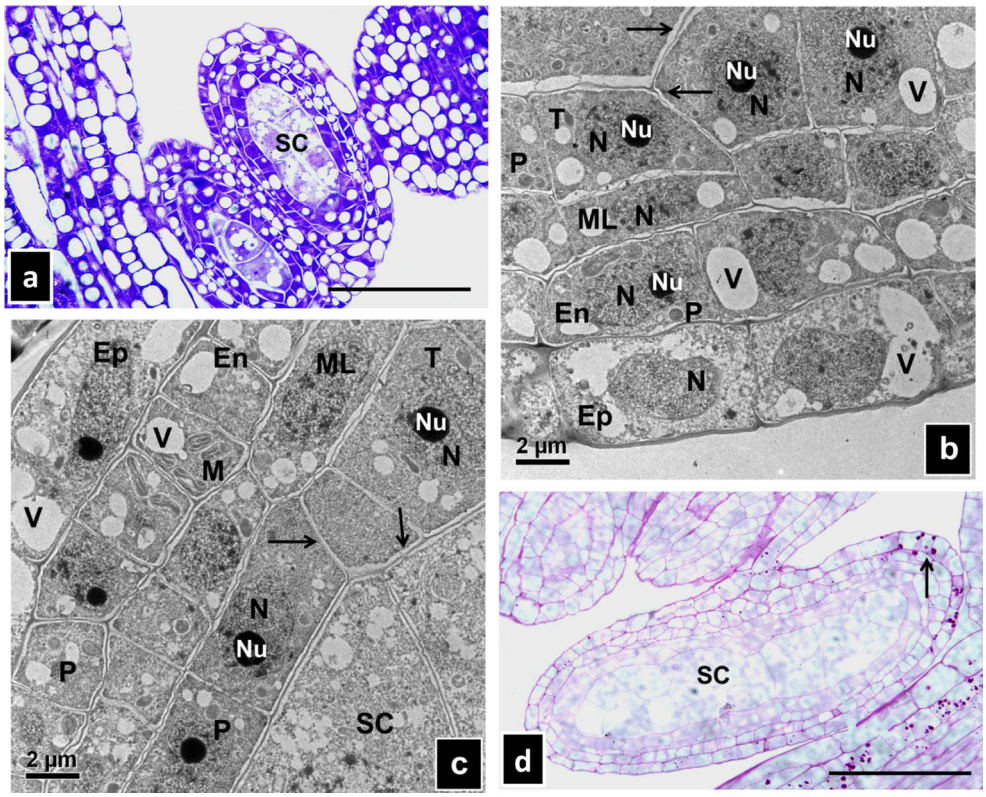

Fig. 5 Light and TEM micrographs of longitudinal sections of spikelets at sporogenous cell stage. **a** Semi-thin section stained with toluidine blue showing sporogenous cells surrounded by four anther layers. **b**, **c** Ultrastructure of developing anther wall at sporogenous cell stage. Note the differentiation of anther into four layers. Plasmodesmata are shown by *arrows*. **d** Semi-thin section stained with PAS. Insoluble polysaccharides are shown by an *arrow*. *Ep* epidermis, *En* endothecium, *ML* middle layer, *T* tapetum, *SC* sporogenous cell, *N* nucleus, *Nu* nucleolus, *V* vacuole, *P* plastid, *M* mitochondrion). Light micrographs: *bar* 50 μm

deposition of insoluble polysaccharides was observed in epidermal cells of the anther wall (Fig. 5d).

Stage 5: Microspore mother cell stage

The sporogenous cells generate microspore mother cells (MMCs). At the microspore mother cell stage of development, the anther wall consists of an epidermis, endothecium, middle layer and a secretory-type tapetum. By the time MMCs complete their development, there is a decline in the cytoplasmic volume of the cells of the middle layer, leading to the collapse of this layer (Fig. 6a, b). However, cytoplasmic connections were still visible between the tapetal cells (Fig. 6b, c). At this stage of development, nuclear divisions were observed in the tapetum with most of the tapetal cells appearing binucleated (Fig. 6a–c). Cytochemical staining showed that insoluble polysaccharides were abundant in the connective tissue of the anther, and some deposition of insoluble polysaccharides was also detected in the epidermal cells (Fig. 6d).

Stage 6: Tetrad stage

Meiotic division of MMCs was accompanied by successive cytokinesis, which resulted in the formation of isobilateral tetrads (Fig. 7a). At this stage of development, the middle layer appeared as a less visible band-like structure (Fig. 7b, c). The tapetal cells were observed as vacuolated and shrunken with darkly stained cytoplasm containing rough ER (Fig. 7b, c). Numerous vacuoles, plastids and mitochondria were observed in epidermal and endothecial cells of the anther wall (Fig. 7b, c). Cytochemical reactions indicated that the connective tissue, epidermis and endothecium of the anther presented a strong reaction with regard to insoluble polysaccharides at the tetrad stage of development (Fig. 7d).

Stage 7: Free microspore stage

Free haploid microspores (Fig. 8a) are released from the tetrads as the callose wall is degraded by callase that is secreted from the tapetal cells. At the free microspore stage, tapetal cells developed as hill-like structures, and characteristic Orbicules/Ubisch bodies were observed on the tangential surface of tapetal cells (Fig. 8b). Ubisch bodies developed osmiophilic spikes (Fig. 8b). The middle layer became more degenerated, and endothecial cells became highly vacuolated (Fig. 8b). Cytochemical tests showed that insoluble polysaccharides were still abundant in the connective tissue of the anther even though they had disappeared in the anther walls at this stage (Fig. 8c, d).

Stage 8: Vacuolated microspore stage

As development progresses, microspores became vacuolated (Fig. 9a) and tapetal cells became more degenerated

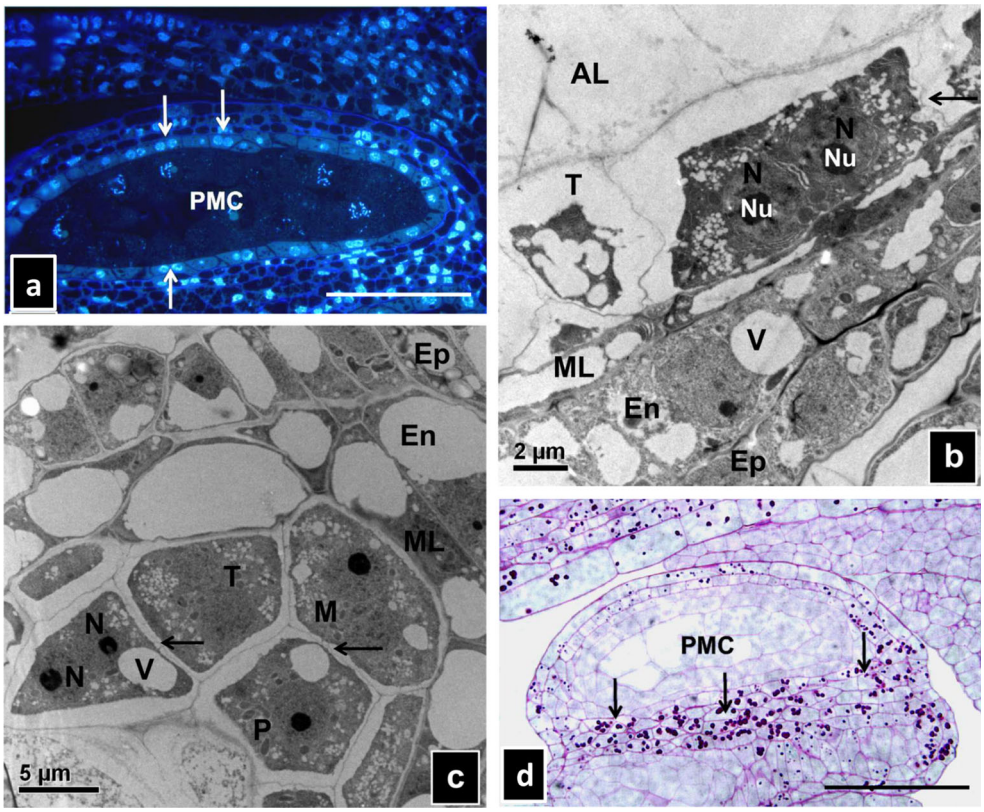

Fig. 6 Light, fluorescent and TEM micrographs of longitudinal sections of spikelets at microspore mother cell stage. **a** Semi-thin section stained with DAPI. Note the presence of binucleated tapetal cells (*arrows*). **b**, **c** Ultrastructure of developing anther wall at microspore mother cell stage. Tapetal cell details with cytoplasmic connections (*arrows*) and nuclear division. Note the binucleated tapetal cells. **d** Semi-thin section stained with PAS. The insoluble polysaccharide content of the anther wall is shown by *arrows*. *Al* anther locule, *Ep* epidermis, *En* endothecium, *ML* middle layer, *T* tapetum, *PMC* pollen mother cell, *N* nucleus, *Nu* nucleolus, *V* vacuole, *P* plastid. Light micrographs: *bar* 50 μm

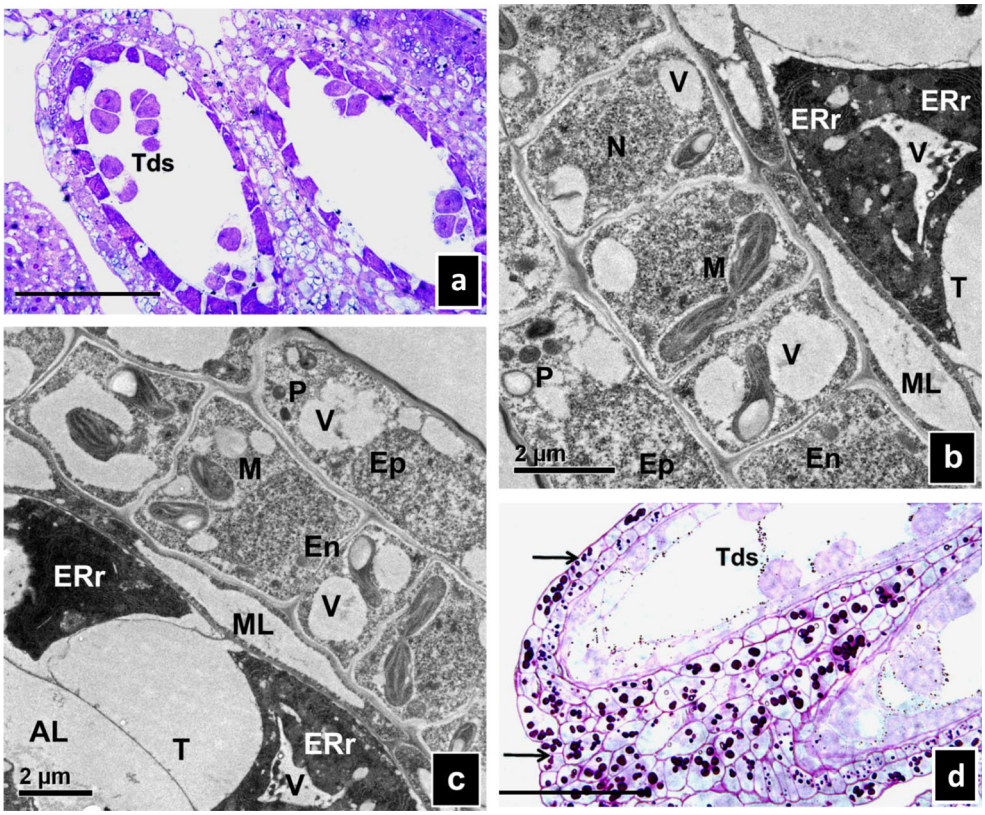

Fig. 7 Light and TEM micrographs of longitudinal sections of spikelets at tetrad stage. **a** Semi-thin section stained with toluidine blue showing tetrads in the anther locule. **b**, **c** Ultrastructure of developing anther wall at tetrad stage. Note the vacuolated, darkly stained and shrunken tapetal cells. Note the presence of ERr in the cytoplasm of tapetal cells. **d** Semi-thin section stained with PAS. The insoluble polysaccharide content of the anther wall is shown by *arrows*. *Al* anther locule, *Tds* tetrads, *Ep* epidermis, *En* endothecium, *ML* middle layer, *T* tapetum, *N* nucleus, *Nu* nucleolus, *V* vacuole, *P* plastid, *ERr* rough endoplasmic reticulum, *M* mitochondrion. Light micrographs: *bar* 50 μm

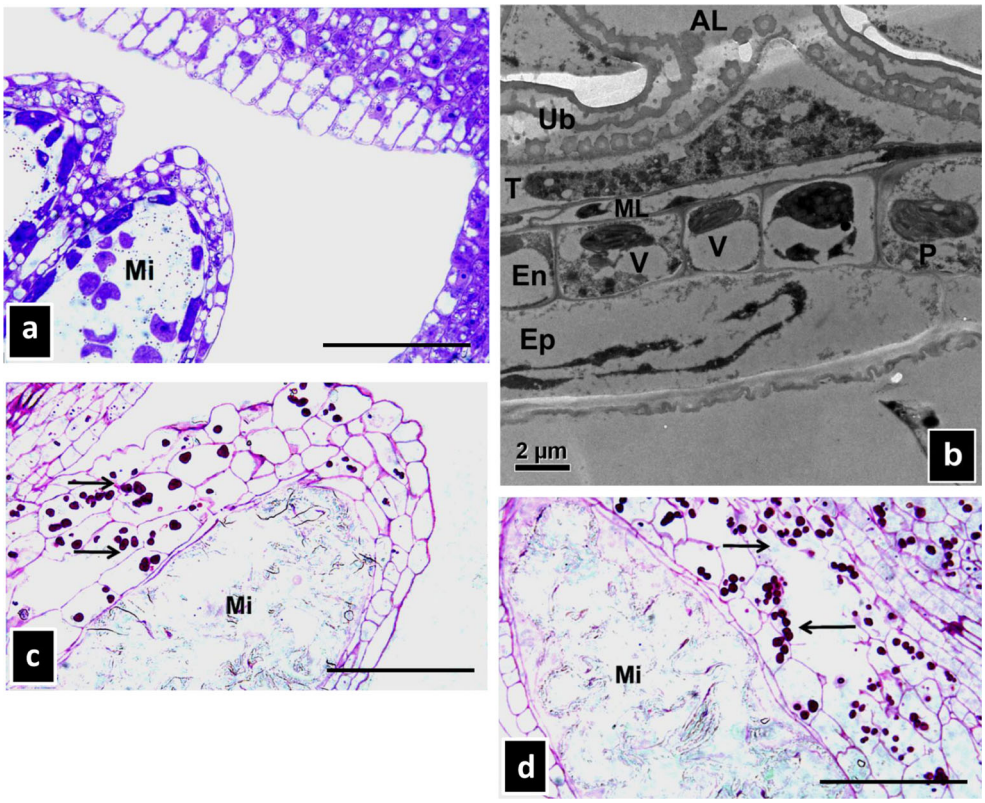

Fig. 8 Light and TEM micrographs of longitudinal sections of spikelets at free microspore stage. **a** Semi-thin section stained with toluidine blue. **b** Ultrastructure of developing anther wall at free microspore stage. Note the formation of hill-like tapetal cells and Ubisch bodies. **c**, **d** Semi-thin section stained with PAS. The insoluble polysaccharide content of the anther wall is shown by *arrows*. *Al* anther locule, *Mi* microspores, *Ep* epidermis, *En* endothecium, *ML* middle layer, *T* tapetum, *V* vacuole, *Ub* Ubisch bodies. Light micrographs: *bar* 50 µm

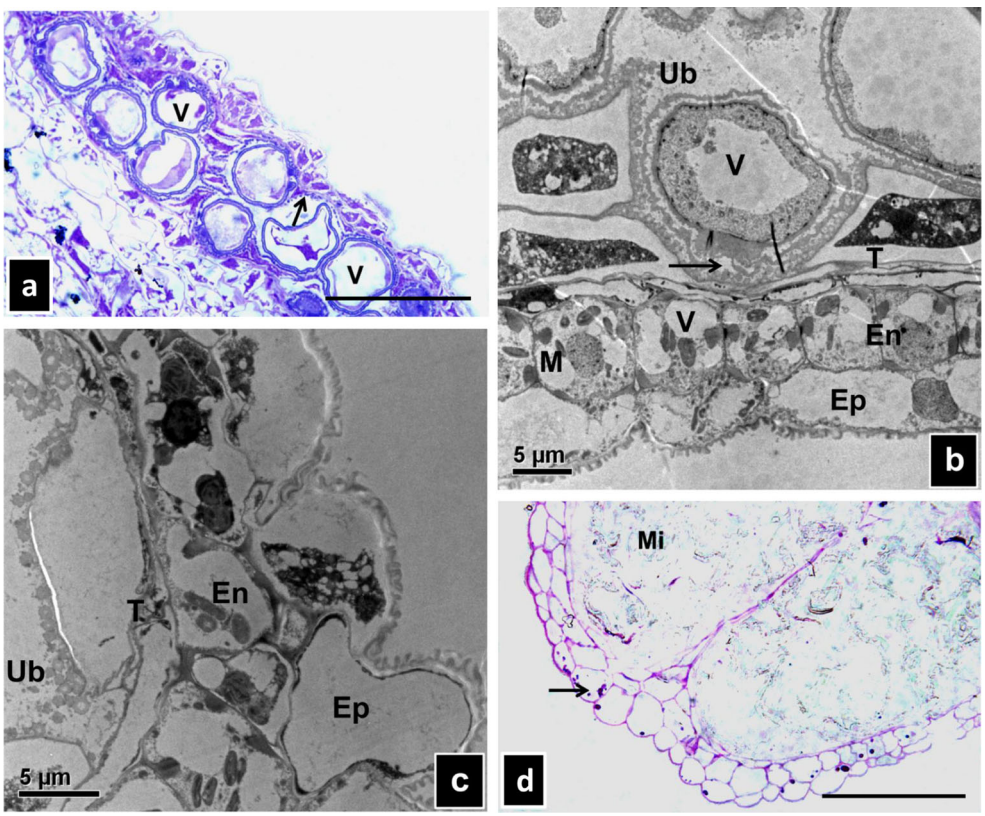

Fig. 9 Light and TEM micrographs of longitudinal sections of anthers at vacuolated microspore stage. **a** Semi-thin section stained with toluidine blue. Note that the tapetum shows the same staining reaction as the exine of microspores (*arrow*) **b**, **c** Ultrastructure of developing anther wall at vacuolated microspore stage. Note the orientation of the pore of microspore towards the tapetum (*arrow*) and accumulation of Ubisch bodies on the tapetal wall. **d** Semi-thin section stained with PAS. The insoluble polysaccharide content of the anther wall is shown by an *arrow*. *Mi* microspore, *Ep* epidermis, *En* endothecium, *T* tapetum, *V* vacuole, *Ub* Ubisch bodies, *M* mitochondrion. Light micrographs: *bar* 50 µm

and formed more electron-dense Ubisch bodies (Fig. 9b, c). Ubisch bodies are fully formed, and their deposition along the tangential surface of the tapetum is complete at this stage. At this stage, the contact between tapetal deposition and pollen exine was clearly visible at the ultrastructure level (Fig. 9b). The middle layer completely disintegrated and became invisible (Fig. 9b, c). Cytochemical test for insoluble polysaccharides carried out by PAS staining revealed a weak reaction in the cells of the anther wall (Fig. 9d).

Stage 9: Bicellular pollen grain

Bicellular pollen grains have well-developed pollen walls (Fig. 10a). During this stage, the tapetal cells almost completely disintegrate into cellular debris and Ubisch bodies on the internal surface (Fig. 10b, c). Ultrastructural studies showed that the epidermal cells formed a layer of cuticle with projections or ridges, and the endothecial cells began to develop fibrous bands (Fig. 10b, c). According to cytochemical studies, bicellular pollen grains showed the accumulation of starch in their cytoplasm (Fig. 10d). However, in this stage, the anther walls (epidermis and endothecium) showed a complete disappearance of insoluble polysaccharides (Fig. 10d).

Stage 10: Mature pollen grain

At this stage of development, pollen grains became more spherical and were completely engorged with reserve substances (starch and lipids) (Fig. 11a). With maturation, the epidermis and endothecium layers degenerated, and the tapetum completely disappeared with only some remnants of Orbicules/Ubisch bodies (Fig. 11b). After degradation of the tapetum, the epidermis and a single row of rectangular-shaped endothecium existed in the mature anther (Fig. 11b), although cells of the latter were observed partially disorganised by the expanding anther wall (Fig. 11c). Cytochemical reactions showed that the epidermis and endothecium were completely devoid of insoluble polysaccharides, and only the remains of insoluble polysaccharides were observed in the connective tissue of the anther (Fig. 11d).

Discussion

This is the first report on anther ontogeny in *B. distachyon*, an emerging model system for diverse and economically important grain, forage and turf crops. The pattern of anther development in *B. distachyon* as reported in this study is the typical monocotyledonous type, where the outer secondary parietal

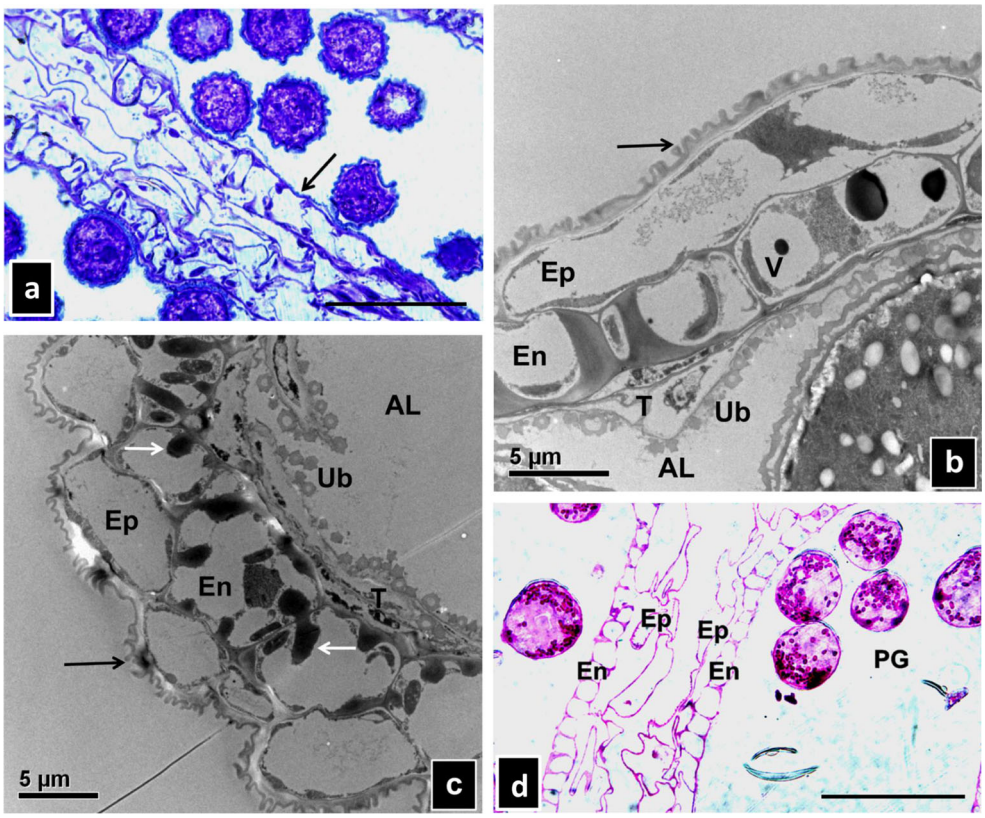

Fig. 10 Light and TEM micrographs of longitudinal sections of anthers at bicellular pollen stage. **a** Semi-thin section stained with toluidine blue. Note the degenerating tapetum (*arrow*). **b**, **c** Ultrastructure of developing anther wall at bicellular pollen stage. Degenerating tapetal cells and Ubisch bodies accumulated on the tapetal wall. Note the formation of projections lining the epidermal cells (*black arrows*) and the formation of fibrous bands in endothecial cells (*white arrows*). **d** Semi-thin section stained with PAS. Note the absence of insoluble polysaccharides in anther walls as evident by negative PAS staining. *Al* anther locule, *Ep* epidermis, *En* endothecium, *T* tapetum, *V* vacuole, *Ub* Ubisch bodies, *PG* pollen grain. Light micrographs: *bar* 50 µm

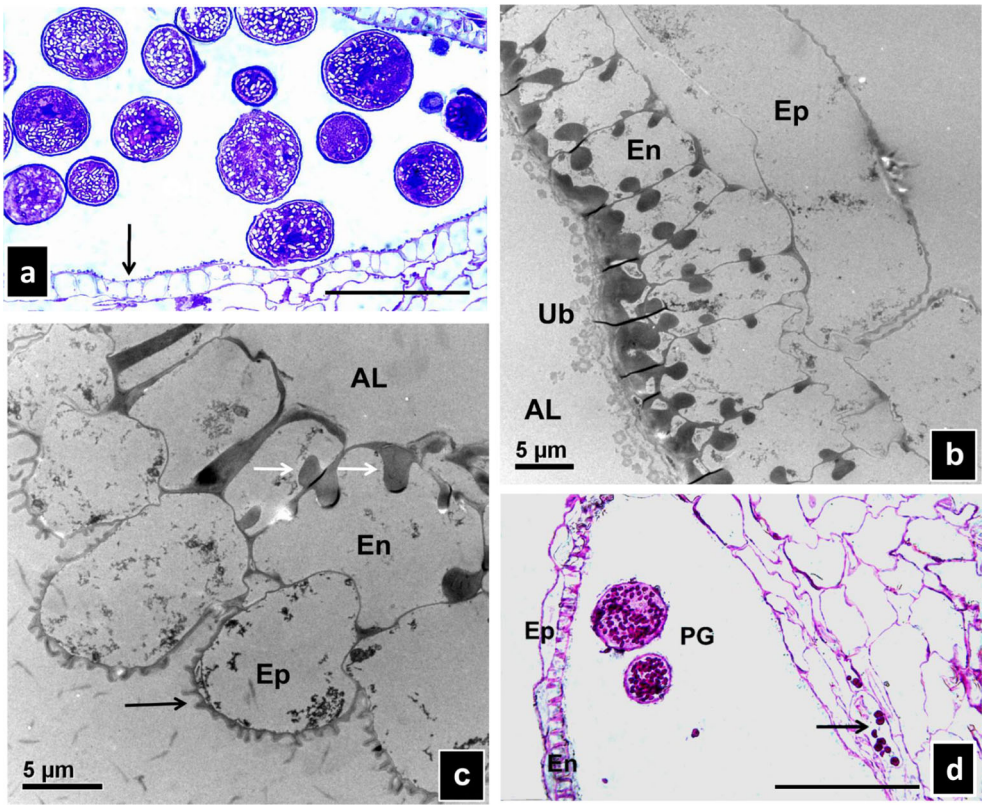

Fig. 11 Light and TEM micrographs of longitudinal sections of anthers at mature pollen stage. **a** Semi-thin section stained with toluidine blue. Only the remains of tapetum left (*arrow*). **b**, **c** Ultrastructure of developing anther wall at mature pollen stage. Note the remnants of Ubisch bodies and disappearance of tapetum. **c** Only the epidermis and endothecium layers are left. Note the presence of projections lining the epidermal cells (*black arrows*) and the fibrous bands in endothecial cells (*white arrows*). **d** Semi-thin section stained with PAS. Note the remains of insoluble polysaccharides in the connective tissue (*arrow*). *Al* anther locule, *PG* pollen grain, *Ep* epidermis, *En* endothecium, *Ub* Ubisch bodies. Light micrographs: *bar* 50 µm

layer develops into the endothecium, and the inner secondary parietal layer generates a middle layer and the tapetum. This type of anther developmental progression is a common feature of members that belong to the Poaceae family (Bhanwra 1988; Teng et al. 2005).

In *B. distachyon*, the wall of young anthers consists of an epidermis, endothecium, middle layer and tapetum. However, at maturity, it comprises only an epidermis and endothecium. Our results are consistent with the results reported in Poaceae, in general, and demonstrate that the anther wall is thin and is composed of four layers of cells (Bhanwra 1988). Our study showed that the endothecial cells became highly vacuolated at the free microspore stage of development and developed fibrous bands at the bicellular stage. The middle layer is made up of rectangular cytoplasmic cells; however, during the microspore mother cell stage of development, these cells become compressed and disorganised. Eventually, cells of the middle layer begin to disappear at the vacuolated microspore stage. These developmental events in the endothecium and the middle layer are similar to those reported earlier in rice (Raghavan 1988).

The most conspicuous and significant layer of the anther tissue is the tapetum. The tapetum in *B. distachyon* is first recognisable at the sporogenous cell stage of anther development and is of the secretory-type, which is typical of grasses (Maheshawari 1950). The secretory-tapetum is considered primitive because of its widespread occurrence in gymnosperms and angiosperms (Johri et al. 1992). During meiosis of microsporocytes, the *Brachypodium* tapetal cells became binucleated (Fig. 6a, b), similar to wheat (Mizelle et al. 1989) and rice (Raghavan 1988). As observed in the present study, tapetal cells were rectangular in outline (Fig. 5b, c) and connected to each other and to the sporogenous cells by cytoplasmic connections, the plasmodesmata. It has been suggested (Heslop-Harrison 1964) that the cytoplasmic connections provide a channel for the rapid transport of nutrients through the sporogenous tissue. The rectangular contour of tapetal cells was correlated with the normal pattern of pollen development, whereas elongated tapetal cells were correlated with pollen abortion (Mizelle et al. 1989). The cells of the secretory tapetum maintain their position and undergo programmed cell death (PCD) during degeneration towards the end of pollen development (Papini et el. 1999; Wu and Cheung 2000). However, the time of degeneration varies greatly from species to species. In *B. distachyon*, the tapetal cells underwent degeneration at the tetrad stage and degenerated completely at the bicellular pollen stage, consistent with the results reported in rice (Zhang et al. 2011). However, in wheat, Mizelle et al. (1989) reported that senescence in tapetal cells begins during the vacuolated microspore stage. The degeneration of the tapetum has been speculated to be a process that makes extra nutrients available to the developing pollen (Pacini 1997, 2010), but it is also important for the occurrence of normal dehiscence of the anther. In a recent

study, Solis et al. (2014) reported the involvement of epigenetic mechanisms accompanying cellular degradation of tapetum via programmed cell death (PCD) event during the late stages of microspore development. The dynamics of DNA methylation was particularly characterized during PCD of tapetal cells in two species, *Brassica napus* and *Nicotiana tabacum*, that indicated existence of epigenetic marks regulating tapetum degradation. The study provides new insights to understand the mechanism of PCD event in tapetal cells, and it will be interesting to know whether similar epigenetic marks are present during tapetal degradation in monocot plants like *Brachypodium*.

One of the main characteristics of secretory tapeta is the production of Orbicules/Ubisch bodies. Ubisch bodies (Orbicules) are granules of sporopollenin lining in the inner tangential and sometimes in the radial walls of tapetal cells (Heslop-Harrison and Dickinson 1969; Hesse 1986; Huysmans et al. 1998) during pollen development. Currently, several reports are available on the structure and development of Ubisch bodies. In rice, Zhang et al. (2011) reported that the tapeta produce characteristic Orbicules/Ubisch bodies that export sporopollenin precursors to the locule. In wheat, El-Ghazaly and Jensen (1986) showed that pre-Ubisch bodies, produced in tapetal cells, formed the core of the Ubisch bodies on which sporopollenin was deposited. Risueno et al. (1969) reported the formation of pro-Ubisch bodies prior to synthesis of sporopollenin granules in the cisternae of the endoplasmic reticulum in the tapetal cytoplasm. Earlier investigations have concluded that the precursors of Ubisch bodies arise as lipoidal bodies in association with rough ER in the tapetal cytoplasm (Rowley 1963; Heslop-Harrison and Dickinson 1969; Christensen et al. 1972; El-Ghazaly and Jensen 1986; Shivanna 2003).

In *B. distachyon*, we observed that the tapetum cell walls start to degrade at the tetrad stage, and the tapetal cells contain abundant rough ER (Fig. 7b, c). Subsequently, Ubisch bodies/Orbicules were observed lining the inner wall of the tapetum (Fig. 8b). This observation signifies the involvement of the rough ER in the synthesis of Ubisch bodies/Orbicules. The next developmental stage begins with vacuolation in the cytoplasm of microspores; numerous Ubisch bodies/Orbicules were observed at the inner tangential wall of the tapetum and showed the same electron density as the sporopollenin observed inside the anther locule (Fig. 9b). Thus, our study in *B. distachyon* supports published observations that the Ubisch bodies/Orbicules originate from the tapetum and are involved in exine synthesis.

In this paper, we also studied the distribution of insoluble polysaccharides in the anther wall of *B. distachyon* during its ontogeny. Anther reserve metabolites are believed to provide energy for tapetum and microspore development (Pacini 2010). During anther development, the distribution of insoluble polysaccharides in the anther correlates with the different stages of male gametophyte development. In developing anther tissues, insoluble polysaccharides are found in the form of a PAS-positive tinge in the cytoplasm, starch storage and cell thickenings (Clèment et al. 1994). As observed until the sporogenous cell stage (Fig. 5d), the amount of insoluble polysaccharides present in the anther walls was negligible. This should be correlated with the fact that these storage polysaccharides provide building blocks for the development and differentiation of anther walls. At the microspore mother cell and tetrad stages of development, large amounts of starch reserves were detected in the epidermis, endothecium and connective tissue of the anther (Figs. 6d and 7d). However, in free microspore and vacuolated microspore stages of development, there was a decline in the amount of insoluble polysaccharides in the connective tissue. At the mature stages (bicellular and mature pollen grain), insoluble polysaccharides were completely absent from the anther wall and connective tissue (Figs. 10d and 11d). However, numerous starch grains were observed in the cytoplasm of pollen grains that correspond to the fact that they are not consumed by the fully grown anther and will be used by the pollen during germination. Our study shows that in *B. distachyon*, sugar synthesis, storage and mobilisation occur in the connective tissue and the layers of the anther wall (i.e. the epidermis, endothecium, middle layer and tapetum) throughout the process of anther and pollen development, and products of starch mobilisation in the anther wall are transported to the locule via the tapetum layer, where they are used for pollen metabolism.

Acknowledgments We thank Dr. Simon Crawford for technical guidance with electron microscopy and access to Advanced Microscopy Facility, The University of Melbourne. AS also thanks Dr. Martin O'Brien for helping in identifying the stages of anther and pollen development and Dr. Lim Chee Liew for helping in organizing the figures during manuscript preparation. Financial support from the Australian Research Council (ARC DPO988972) is also gratefully acknowledged.

Conflict of interest The authors declare that they have no conflict of interest.

References

Alves SC, Worland B, Thole V, Snape JW, Bewan MW, Vain P (2009) A protocol for *Agrobacterium*-mediated transformation of *Brachypodium distachyon* community standard line Bd21. Nat Protoc 4:638–649

Aybeke M (2012) Anther wall and pollen development in *Ophrys mammosa* L. (Orchidaceae). Plant Syst Evol 298:1015–1023

Bedinger PA (1992) The remarkable biology of pollen. Plant Cell 4:879–887

Bevan MW, Garvin DF, Vogel JP (2010) *Brachypodium distachyon* genomics for sustainable food and fuel production. Curr Opin Biotech 21:211–217

Bhandari NN (1984) The microsporangium. In: Johri BM (ed) The embryology of angiosperms. Springer, Berlin, pp 53–157

Bhanwra RK (1988) Embryology in relation to systematic of Gramineae. Ann Bot 62(2):215–233

Carrizo Garcia C (2002) Anther wall formation in *Solanaceae* species. Ann Bot 90:701–706

Christensen JE, Horner HT, Lersten NR (1972) Pollen wall and tapetal orbicular wall development in *Sorghum bicolour* (Graminae). Am J Bot 59:43–58

Clèment C, Chavant L, Burrus M, Audran JC (1994) Anther starch variations in *Lilium* during pollen development. Sex Plant Reprod 7:347–356

Datta R, Chamusco KC, Chourey PS (2002) Starch biosynthesis during pollen maturation is associated with altered patterns of gene expression in maize. Plant Physiol 130:1645–1656

Davis GL (1996) Systematic embryology of the angiosperms. Wiley, New York

Dorion S, Lalonde S, Saini HS (1996) Induction of male sterility in wheat by meiotic stage water deficit is preceded by a decline in invertase activity and changes in carbohydrate metabolism in anthers. Plant Physiol 111:137–145

Draper J, Mur LA, Jenkins G, Ghosh-Biswas GC, Bablak P, Hasterok R, Routledge AP (2001) *Brachypodium distachyon*. A new model system for functional genomics in grasses. Plant Physiol 127: 1539–1555

El-Ghazaly G, Jensen WA (1986) Studies of the development of wheat (*Triticum aestivum*) pollen. I Formation Pollen Wall Ubisch Bodies Grana 25:1–29

Garvin DF, Gu YQ, Hasterok R, Hazen SP, Jenkins G, Mockler TC, Mur LAJ, Vogel JP (2008) Development of genetic and genomic research resources for *Brachypodium distachyon*, a new model system for grass crop research. Crop Sci 48:S69–S84

Hardy CR, Stevensen DW (2000) Development of the gametophytes, flower and floral vasculature in *Cochliostema odoratissumum* (Commelinaceae). Bot J Linn Soc 134:131–157

Heslop-Harrison J (1964) Cell walls, cell membranes and protoplasmic connections during meiosis and pollen development. In: Linskens HF (eds) Pollen physiology and fertilization. Amsterdam, North-Holland, pp 39–47

Heslop-Harrison J, Dickinson MC (1969) Fine relationship of sporopollenin synthesis associated with tapetum and microspore in *Lilium*. Planta 84:199–214

Hesse M (1986) Orbicules and the ektexine are homologous sporopollenin concretions in Spermatophyta. Plant Syst Evol 153:37–48

Hong SY, Park JH, Cho SH, Yang MS, Park CM (2011) Phenological growth stages of *Brachypodium distachyon*: codification and description. Weed Res. doi:10.1111/j.1365-3180.2011.00877.x

Huysmans S, El-Ghazaly G, Smets E (1998) Orbicules in angiosperms: morphology, function, distribution, and relation with tapetum type. Bot Rev 64:240–272

Johri BM, Ambegaokar KB, Srivastava PS (1992) Comparative embryology of Angiosperms, vol 1. Springer, Berlin, pp 504–509

Liu CC, Huang TC (2003) Anther and pollen wall development in *Dumasia miaoliensis* Liu and Lu (Fabaceae). Taiwania 48:273–281

Maheshwari P (1950) An introduction to the embryology of angiosperms. McGraw-Hill, New York

Mascarenhas JP (1989) The male gametophyte of flowering plants. Plant Cell 1:657–664

Mizelle MB, Sethi R, Ashton ME, Jensen WA (1989) Development of the pollen grain and tapetum of wheat (*Triticum aestivum*) in untreated plants and plants treated with chemical hybridizing agent RH0007. Sex Plant Reprod 2:231–253

Opanowicz M, Vain P, Draper J, Parker D, Doonan JH (2008) *Brachypodium distachyon*: making hay with a wild grass. Trends Plant Sci 13:172–177

Pacini E (1990) Tapetum and microspore function. In: Blackmore S, Knox RB (eds) Microspores: evolution and ontogeny. Academic, London, pp 213–237

Pacini E (1997) Tapetum character states: analytical keys for tapetum types and activities. Can J Bot 75:1448–1459

Pacini E (2000) From anther and pollen ripening to pollen presentation. Plant Syst Evol 222:19–43

Pacini E (2010) Relationships between tapetum, loculus, and pollen during development. Int J Plant Sci 171:1–11

Pacini E, Franchi GG, Hesse M (1985) The tapetum: its form, function, and possible phylogeny in Embryophyta. Plant Syst Evol 149:155–185

Papini A, Mosti S, Brighigna L (1999) Programmed cell death events during tapetum development of angiosperms. Protoplasma 207: 213–221

Polowick PL, Sawhney VK (1992) Ultrastructural changes in the cell wall, nucleus and cytoplasm of pollen mother cells during meiotic prophase I in *Lycopersicum esculentum* (Mill.). Protoplasma 169: 139–147

Raghavan V (1988) Anther and pollen development in rice (*Oryza sativa*). Am J Bot 75:183–196

Risueno MC, Gimenez-Martin G, Lopez-Saez JF, Garcia MIR (1969) Origin and development of sporopollenin bodies. Protoplasma 67: 361–374

Rowley JR (1963) Ubisch body development in *Poa annua*. Grana Palynol 4:25–36

Sato T (1968) A modified method for lead staining of thin sections. J Electr Microsc, Tokyo 17:158–159

Schrauwen JAM, Mettenmeyer T, Croes AF, Wullems GJ (1996) Tapetum-specific genes: what role do they play in male gametophyte development. Acta Bot Neerl 45:1–15

Sharma A, Singh MB, Bhalla PL (2014) Cytochemistry of pollen development in *Brachypodium distachyon*. Plant Syst Evol. doi:10.1007/s00606-014-0989-9

Shivanna KR (2003) Pollen biology and biotechnology. Science, New Hampshire

Solís MT, Chakrabarti N, Corredor E, Cortés-Eslava J, Rodríguez-Serrano M, Biggiogera M, Risueno MC, Testillano PS (2014) Epigenetic changes accompany developmental programmed cell death in tapetum cells. Plant Cell Physiol 55(1):16–29

Teng N, Huang Z, Xijin M, Jin B, Hu Y, Lin J (2005) Microsporogenesis and pollen development in *Leymus chinensis* with emphasis on dynamic changes in callose deposition. Flora 200:256–263

Vogel J, Hill T (2008) High-efficiency *Agrobacterium*-mediated transformation of *Brachypodium distachyon* inbred line Bd21-3. Plant Cell Rep 27:471–478

Wu HM, Cheung AY (2000) Programmed cell death in plant reproduction. Development 44:267–281

Zhang D, Luo X, Lu Z (2011) Cytological analysis and genetic control of rice anther development. J Genet Genomics 38:379–390